HHS Public Access

Author manuscript

Int J Radiat Oncol Biol Phys. Author manuscript; available in PMC 2022 July 01.

Published in final edited form as:

Int J Radiat Oncol Biol Phys. 2021 July 01; 110(3): 792–803. doi:10.1016/j.ijrobp.2021.01.033.

A Phase II Study of Dose-Intensified Chemoradiation Using Biologically-Based Target Volume Definition in Patients with Newly Diagnosed Glioblastoma

Michelle M. Kim, MD[1], **Yilun Sun, PhD**[1,2], **Madhava P. Aryal, PhD**[1], **Hemant A. Parmar, MD**[3], **Morand Piert, MD**[3], **Benjamin Rosen, PhD**[1], **Charles S. Mayo, PhD**[1], **James M. Balter, PhD**[1], **Matthew Schipper, PhD**[1,2], **Nicolette Gabel, PhD**[4], **Emily M. Briceño, PhD**[4], **Daekeun You, PhD**[1], **Jason Heth, MD**[5], **Wajd Al-Holou, MD**[5], **Yoshie Umemura, MD**[6], **Denise Leung, MD**[6], **Larry Junck, MD**[6], **Daniel R. Wahl, MD, PhD**[1], **Theodore S. Lawrence, MD, PhD**[1], **Yue Cao, PhD**[1,3,7]

[1.]The University of Michigan, Department of Radiation Oncology, Ann Arbor, Michigan

[2.]The University of Michigan, Department of Biostatistics, Ann Arbor, Michigan

[3.]The University of Michigan, Department of Radiology, Ann Arbor, Michigan

[4.]The University of Michigan, Department of Physical Medicine and Rehabilitation, Ann Arbor, Michigan

[5.]The University of Michigan, Department of Neurosurgery, Ann Arbor, Michigan

[6.]The University of Michigan, Department of Neurology, Ann Arbor, Michigan

[7.]The University of Michigan, Department of Biomedical Engineering, Ann Arbor, Michigan

Abstract

Purpose/Objectives: We hypothesized that dose-intensified chemoradiation (chemoRT) targeting adversely prognostic hypercellular (TV_{HCV}) and hyperperfused (TV_{CBV}) tumor volumes would improve outcomes in patients with glioblastoma (GBM).

Materials/Methods: This single-arm phase II trial enrolled adult patients with newly diagnosed GBM. Patients with >1cc TV_{HCV}/TV_{CBV} identified using high b-value diffusion-weighted MRI and dynamic contrast-enhanced perfusion MRI were treated over 30 fractions to 75 Gy to the TV_{HCV}/TV_{CBV} with temozolomide. The primary objective was to estimate improvement in 12-month overall survival (OS) versus historical control. Secondary objectives included evaluating the effect of 3-month TV_{HCV}/TV_{CBV} reduction on OS using Cox proportional-hazard regression, and characterizing coverage (95%IDL) of metabolic tumor volumes (MTV) identified using correlative

Corresponding author: Michelle M. Kim, MD; University of Michigan, Department of Radiation Oncology, 1500 E. Medical Center Dr., Ann Arbor, MI 48109-0010; Phone:(734)647-8946; Fax:(734)763-7370; michekim@med.umich.edu.

Conflicts of interest: None

^{11}C-Methionine PET. Clinically meaningful change was assessed for quality of life (QOL) by EORTC-QLQ-C30, symptom burden by MDASI-BT, and neurocognitive function (NCF) by COWA, Trail Making Test A/B, and HVLT-R.

Results: Between 2016–2018, 26 patients were enrolled. Initial patients were boosted to TV_{HCV} alone, and 13 patients to both TV_{HCV}/TV_{CBV}. Gross or subtotal resection was performed in 87% of patients, 22% were MGMT methylated. With 26-month follow-up (95%CI 19-NR), among patients boosted to the combined TV_{HCV}/TV_{CBV} 12-month OS was 92% (95%CI 78–100%, p=0.03) and median OS was 20 months (95%CI 18-NR), and OS 20 months (95%CI 14–29) for the whole study cohort. Patients whose 3-month TV_{HCV}/TV_{CBV} decreased to <median (3 cc) had superior OS (29 vs 12 months, p=0.02). Only 5 patients had central or in-field failures, and 93% (IQR 59–100) of the ^{11}C-Methionine MTV received high-dose coverage. Late grade 3 neurologic toxicity occurred in 2 patients. Among non-progressing patients, 1 and 7-month deterioration in QOL, symptoms and NCF were similar in incidence to standard therapy.

Conclusions: Dose-intensification against hypercellular/hyperperfused tumor regions in GBM yields promising OS, particularly among patients with greater tumor reduction 3-months post-RT, with favorable NCF, symptom burden and QOL.

Keywords

Dose-intensified; advanced MRI; radiation therapy; biologically-based; glioblastoma

Introduction

For patients with glioblastoma (GBM), key biologic properties identified by advanced imaging techniques predict outcome better than anatomic MRI, but no such imaging biomarker has been integrated into standard treatment for this lethal disease.[1] The development of imaging biomarkers that enable spatial identification and temporal monitoring of a therapy resistant phenotype prior to, during and after treatment is an important first step towards improving outcomes in patients with GBM. However, efforts to seamlessly incorporate advanced imaging modalities into radiation treatment planning have thus far only been limited to centers with robust technical expertise.

In contrast to more specialized studies, most centers routinely perform perfusion as well as diffusion-weighted MRI (DW-MRI) for the assessment of brain tumor patients. Perfusion, quantified from dynamic susceptibility contrast (DSC) and dynamic contrast enhanced (DCE) MRI, can assess elevation of cerebral blood volume (CBV) and cerebral blood flow (CBF) associated with neovascularization and tumor growth that predict worse PFS and OS.[2–6] Diffusion MRI (b=0–1000 s/mm^2) estimates water mobility in the tissue microenvironment as an indicator of tumor cellularity, [7–10] and by extending the degree of diffusion-weighting to a high b-value (b=3000 s/mm^2), distinguishes high-density cellular tumor regions from normal brain tissue, edema and micronecrosis and predicts recurrence and PFS.[11] Using these widely available techniques, we demonstrated that combining DCE MRI with high b-value DW-MRI identifies largely unique, non-overlapping hyperperfused (TV_{CBV}) and hypercellular (TV_{HCV}) tumor volumes that spatially predict patterns of failure

better than either technique alone, and nearly always contain treatment-resistant disease that will progress.[11, 12]

In a prior institutional phase I/II study[13], we demonstrated that dose-intensified targeting of tumor regions using conventional, anatomic imaging and conformal planning techniques with concurrent temozolomide was safe and potentially effective. Consistent with other studies, tumor was identified outside of the standard enhancing boost target using ^{11}C-Methionine (^{11}C-MET) PET, which was associated with an increased risk of non-central tumor failure.[13] Recognizing the limitations of conventional, anatomic MRI to adequately define biologically relevant tumor, we sought to implement a potentially generalizable advanced imaging technique utilizing DCE- and high b-value DW-MRI that was prognostic for tumor recurrence and that could be feasibly integrated into the radiation treatment planning process.[14] Because standard-of-care tumor volumes often do not include part of the adversely prognostic tumor regions identified by DCE- and high b-value DW-MRI[11, 12], we hypothesized that specifically targeting these tumor regions with dose-intensified chemoradiation would improve patient outcomes. We report the results of a phase II study implementing an advanced, multiparametric MRI technique enabling selective targeting of hyperperfused and hypercellular tumor with dose-escalated radiotherapy in patients with GBM.

Methods

This phase II, single-institution, single arm trial was approved by the Michigan institutional review board and registered at ClinicalTrials.gov (NCT02805179). Informed consent was required and obtained from all patients.

Patient eligibility

Adult patients with newly diagnosed, histologically-confirmed supratentorial WHO grade IV glioblastoma and gliosarcoma were eligible. The maximal contiguous volume of tumor based on advanced MRI was required to be < 1/3 the volume of brain, and patients were required to be registered within 6 weeks of most recent resection. Patients were required to have a Karnofsky Performance Status ≥ 70, life expectancy of at least 12 weeks, and adequate organ function defined as hemoglobin ≥10 g/dL (potentially reached by transfusion), absolute neutrophil count ≥1500/mm^3, platelet count ≥100,000/mm^3, total bilirubin ≤2 times the upper limit of normal (unless elevated due to Gilbert syndrome), ALT/AST ≤5 times the upper limit of normal, and serum creatinine ≤2.0 mg/dL within 14 days prior to registration. Exclusion criteria included recurrent glioma, prior use of carmustine wafers or similar intratumoral or intracavitary treatment, multifocal disease defined as >1 lobe of discontiguous, contrast enhancing disease based on T1-weighted gadolinium enhanced MRI, or evidence of leptomeningeal dissemination. Additional exclusion criteria included prior chemotherapy within 3 years, prior invasive malignancy unless disease-free for a minimum of 3 years, severe concurrent disease requiring treatment, or prior cranial radiotherapy with significant overlap. Patients unable to undergo MRI scans were excluded, and a negative pregnancy test within 14 days prior to registration was required.

Pre-radiation advanced imaging

MR simulation—In addition to CT simulation with immobilization in a thermoplastic mask, all patients underwent an MRI simulation in the Department of Radiation Oncology on a 3.0 Tesla scanner (Skyra, Siemens Healthineers, Erlangen, Germany) using a 20-channel head coil. Anatomic 3-dimensional (3D) pre- and post-contrast T1-weighted images and 2-dimensional T2-FLAIR images were acquired. Additionally, DW-MR images were acquired using a 2D RESOLVE pulse sequence with diffusion weighting in 3 orthogonal directions and b-values of 0 and 3000 s/mm^2. DCE-MR images were acquired by a 3D gradient echo pulse sequence called TWIST, in the sagittal orientation to avoid in-flow effect and ensure sufficient arterial coverage for accurate input function measurement as previously described.[14] Hardware and software quality assurance was conducted to ensure accuracy and reproducibility of multipametric MRI for clinical use.[14]

^{11}C-Methionine PET—For secondary analyses, correlative ^{11}C-Methioinine PET imaging was acquired prior to radiation treatment on a Siemens ECAT EXACT HR+ whole body scanner (axial resolution 4.1 mm full width at half maximum in the center of the field of view). Scans were obtained in 3D mode after injection of approximately 740 MBq of ^{11}C MET in a dynamic acquisition. Summed image data obtained between 10–30 minutes after injection were analyzed. The metabolic tumor volume (MTV) was defined by automatic segmentation using a threshold of 1.5 times mean activity of the normal cerebellum, as previously published,[15] and centrally reviewed by the study nuclear radiologist (M.P.).

Processing and generation of hypercellular and hyperperfused tumor volumes

The data transfer and procedural workflow enabling seamless passage of data from the radiation treatment planning system (TPS) to the image processing software and back to the TPS has been previously described.[14] The hyperperfused tumor volume (TV_{CBV}) was delineated on the CBV images using an automated threshold method, and defined as the volume of tumor with CBV greater than 1 SD above contralateral frontal lobe grey matter. The hypercellular tumor volume (TV_{HCV}) was determined directly on the b=3000 s/mm^2 DW images using an automated threshold method, and defined as 2 SD above the mean intensity of contralateral normal brain.[14] Image analysis was performed using in-house software (imFIAT).[16]

Treatment

Radiation treatment planning—Treatment planning was performed using a commercial system (Eclipse version 13.6, Varian Medical Systems, Palo Alto, CA) using volumetric modulated arc therapy. Standard target volumes were generated using anatomic T1-weighted gadolinium-enhanced and T2-FLAIR images. For all patients, the GTV_Low was defined as the surgical cavity and residual contrast enhancement. The CTV_Low was defined as 1.7 cm margin beyond GTV_Low, delimited by anatomic boundaries. No additional CTV margin was added to the T2-FLAIR abnormality, and T2-FLAIR was not specifically targeted although generally included in the CTV_Low. PTV_Low was defined as a 3 mm geometric expansion of CTV_Low, and prescribed 60 Gy in 30 fractions. For 10 patients, GTV_High was defined as the hypercellular tumor volume (TV_{HCV}) derived from the high b-value

DW-MRI. After subsequent analysis[12] demonstrated the improved prognostic value of identifying both hypercellular tumor based on DW-MRI and hyperperfused tumor (TV_{CBV}) based on DCE-MRI, the study was amended and GTV_High was defined as the combination (mathematical union) of both TV_{HCV} and TV_{CBV} for the remaining 13 treated patients. No CTV margin was used to expand the GTV_High. A 5 mm PTV_High margin was used to account for daily setup error (3 mm), MR to CT registration error (1 mm), and distortion correction of the DW-MRI (1 mm). A simultaneous integrated boost technique was used to deliver 75 Gy at 2.5 Gy per fraction over 30 fractions to the PTV_High.

Standard organs at risk (OAR) were delineated with planning risk volumes (PRVs) defined as the organ at risk expanded by 3 mm. When an OAR was adjacent to a PTV, the dose was planned as close as possible to the prescription PTV dose without exceeding normal tissue dose constraints.

Surgery and chemotherapy—Following maximal safe resection, all patients were treated per standard of care with concurrent daily (75 mg/m^2) and adjuvant (150–200 mg/m^2 days 1–5 of a 28-day cycle) temozolomide for 6–12 months or until disease progression or treatment intolerance. Dose-reductions were permitted when clinically indicated, and additional cycles were prescribed at the discretion of the treating physician.

Patient assessments

Imaging—Per standard of care, patients underwent conventional diagnostic MR imaging 1 month post-chemoradiation, and then approximately every 2 months thereafter. Additionally, patients underwent advanced MRI scans including high b-value DW-MRI and DCE-MRI during week 3–4 of radiation, and 3 months post-chemoradiation. All high b-value DW-MRI and DCE-MRI scans were performed on the same 3.0 Tesla scanner in the Department of Radiation Oncology.

Neurologic, quality of life, and neurocognitive function assessments—All patients underwent assessment of neurological status using the Neurologic Assessment in Neuro-Oncology (NANO) Scale[17] pre-radiation and 3 months post-radiation. Additionally, longitudinal assessment of patient-reported symptom burden and interference using MD Anderson Symptom Inventory Brain Tumor (MDASI-BT)[18], and quality of life using the European Organisation for the Research and Treatment of Cancer Quality of Life Questionnaire C30/BN20 (EORTC QLQ-C30/BN20)[19, 20] were assessed pre-radiation, 6 weeks into radiation, and 1 and 7 months post-radiation. Objective neurocognitive function (NCF) was assessed using the Hopkins Verbal Learning Test-Revised[21] (HVLT-R; tests for Total Recall, Delayed Recall, and Delayed Recognition) for learning and memory, the Trail Making Test[22] Part A and Part B for processing speed and executive function, respectively, and the Controlled Oral Word Association[23] (COWA) for verbal fluency. Assessments were performed pre-radiation, and 1 and 7 months post-radiation. All NCF tests were administered by neuropsychology faculty (N.G. and E.B.) and a neuropsychology fellow.

Toxicity—All treatment-emergent adverse events (AE) were graded using CTCAE v. 4.03. Acute toxicities were assessed up to 30 days post-chemoradiation. Subacute and late

neurologic toxicity beyond 30 days was assessed every 2–3 months, and all patients were monitored for late neurologic toxicity until last follow-up or death.

Survival and tumor progression—Overall survival (OS) was defined as the interval from the start of radiation until death, or censored at the date of last follow-up on which the patient was alive. Progression-free survival (PFS) was defined as the interval from the start of RT until progression or death, or censored at the date of last imaging follow-up. Overall survival and PFS were estimated using the Kaplan-Meier method. Patients were routinely followed approximately every 2–3 months after chemoradiation with MRI and for clinical evaluation. In instances where pathologic confirmation was unavailable, progression was adjudicated in a multidisciplinary tumor board and defined as worsening enhancement outside of the radiation field, or within the radiation field based on serial, confirmatory imaging with or without adjunctive advanced imaging including perfusion MRI or MR spectroscopy, when clinically indicated. Response rate was evaluated 3 months post-chemoradiation using Response Assessment in Neuro-oncology (RANO)[24] criteria.

Statistical methods

The primary objective of the study was to determine whether 12-month overall survival rate was significantly improved compared to the reported outcomes of the standard arms of RTOG 0525[25] and RTOG 0825[26], that both included treatment to 60 Gy in 30 fractions based on anatomic MRI. Allowing 10% ineligibility, a sample of 23 patients would provide 80% power to detect a 20% absolute increase in 12-month OS from 65% to 85%, based on an exact 1-sided binomial test at alpha = 0.10.

Secondary objectives included characterization of patterns of recurrence, classified according to the proportion of the recurrence volume contained within the 95% prescription isodose surface (relative to 75 Gy): central (>95%), in-field (>80–95%), marginal (20–08%), or distant (<20%), and assessment of high-dose coverage of the metabolic tumor volume (MTV) defined by correlative ^{11}C-MET PET imaging, which we had previously demonstrated[15] to be associated with non-central tumor recurrence. Additional secondary objectives included characterization of the incidence of acute and late grade 3+ neurologic toxcities, and analysis of post-treatment changes in the hypercellular/hyperperfused tumor volume 3 months post-chemoradiation. The log-rank test was used to compare survival outcomes between patients with and without significant residual hypercellular/hyperperfused tumor.

The proportion of patients experiencing clinically meaningful change in symptoms and quality of life was assessed at the prespecified time points. For the MDASI-BT, a change in symptom severity of one point from baseline, and for the EORTC QLQ-C30/BN20, a difference of 10 points from the baseline measurements were classified as the minimum clinically meaningful change based on previous reports.[27] Neurocognitive status was categorized as improved, stable, or declined using the Reliable Change Index[27, 28] for each test. Neurologic outcome was defined using NANO response criteria.[17]

Statistical analyses were performed using R (version 3.6.1). For all analyses, two-sided p-values of <.05 were considered statistically significant and values <.1 were considered a marginal association. Confidence intervals estimates were two-sided and set at 95%.

Results

Enrollment, patient population and treatment delivery

Between September 2016 and December 2018, 26 patients were enrolled. One patient had insufficient (<1 cc) TV_{CBV} and TV_{HCV} for radiotherapy targeting, and 2 patients were ineligible based on the presence of multifocal enhancing disease. For the primary endpoint, 23 eligible patients treated with dose-intensified chemoradiation were analyzable.

The median age was 61 years (IQR 56–66), and 70% were male. Eighty-seven percent of patients had tumors located in the frontal or temporal lobes, and 65% were left-sided. Accordingly, the most common neurologic function deficits occurred in motor and language domains, although 86% of observed deficits were mild (Table 1). The majority of patients underwent gross total (57%) or subtotal (30%) resection, and 22% of patients had MGMT promoter methylation. All patients were IDH1 wild-type (1 unknown), assessed by immunohistochemistry and confirmed by next generation sequencing if the patient was <55 years old. Only 2 of the 23 patients received adjuvant tumor-treating fields.

All patients except two completed protocol treatment. One patient boosted to the hypercellular tumor alone discontinued after 67.5 Gy in 27 fractions due to clinical decline from tumor progression. A 2nd patient, boosted to the combined hypercellular/hyperperfused tumor, stopped treatment after 67.5 Gy due to symptomatic cerebral edema.

Imaging characteristics

The median hypercellular tumor volume pre-radiotherapy was 6 cc (IQR 4–11), and the median hyperperfused tumor volume was approximately 5 cc (IQR 2–10) (Table 2). Consistent with our prior retrospective analyses, these volumes were largely complementary, with only 0.5 cc overlap. The median combined hypercellular/hyperperfused tumor volume (union of TV_{HCV}/TV_{CBV}) was 11 cc (IQR 7–20), and 35% of the combined TV_{HCV}/TV_{CBV} (IQR 25–57%) was non-enhancing (Table 2). Non-enhancing tumor was identified by both high b-value DW-imaging and CBV maps, and approximately 1/3 of the individual TV_{HCV} and TV_{CBV} tumor volumes were non-enhancing, respectively. Despite identifying a significant volume of non-enhancing disease, the combined TV_{HCV}/TV_{CBV} was on average 30% smaller than the enhancing tumor volume (excluding surgical cavity, 17 cc) (Table 2).

The GTV_Low (residual contrast enhancement plus surgical cavity), representing the standard boost volume and the dose-escalation target of the BN-001 trial, was almost 3 times larger (median 31 cc, IQR 15–51) than the hypercellular/hyperperfused combined TV_{HCV}/TV_{CBV} (11 cc) that was the dose-escalation target on this trial. Still, 34% (IQR 20–59%) or approximately 4 cc (IQR 3–6) of the combined TV_{HCV}/TV_{CBV} extended beyond the GTV_Low. Only 2 cc (IQR 0–11) of the FLAIR volume extended beyond the CTV_Low.

There was no significant difference in the pre-radiation combined hypercellular/hyperperfused tumor volume between MGMT methylated vs unmethylated patients (p=0.2).

Survival

The median follow-up time was 26 months (19-NR). Patients treated to the combined hypercellular/hyperperfused tumor volume had significantly improved 12-month OS (92%, 95% CI 78–100%) compared to historical control (p=0.03). The median OS of this cohort was 20 months (18-NR), and the median PFS was 12 months (10–17 months) (Figure 1, Panel A-B). Among all 23 patients, the median OS was 20 months (95% CI 14–29) (Figure 1, Panel C). There was no significant difference in 12-month OS between patients boosted to the hypercellular tumor volume alone vs historical control (p=0.9).

Three-month response assessment and survival

Among patients with available data without tumor progression three months post-RT, 67% had neurologic stability as defined by NANO response criteria, and 84% were either not taking steroids (11/19) or on stable/decreased (5/19) doses of steroids.

Nineteen patients with available 3-month advanced MR imaging were analyzed for tumor response (excluding 1 patient who had received bevacizumab that could confound analysis of perfusion imaging). By 3 months post-RT, the combined hypercellular/hyperperfused tumor volume (TV_{HCV}/TV_{CBV}) reduced for the majority of patients (median 11 cc to 3 cc) (Table 2). At this time point, 52% (IQR 28–71%) of the residual TV_{HCV}/TV_{CBV} was non-enhancing and comprised a greater proportion of the total TV_{HCV}/TV_{CBV} than pre-radiation (35%). Three patients had no residual TV_{HCV}/TV_{CBV}.

Patients with less than the median (3 cc) residual TV_{HCV}/TV_{CBV} by 3 months post-treatment had significantly improved OS compared to patients with ≥median residual tumor volume (29 vs 12 months, p=0.02) (Figure 2, Panel A). In contrast, the volume of residual contrast-enhancement (excluding surgical cavity) was not significantly associated with survival. Moreover, using RANO response criteria for tumor assessment, 90% of patients were categorized as having stable disease, which could not be used to stratify patient outcome (Figure 2, Panel B).

Patterns of failure and correlation with metabolic tumor volume

Among 16 patients with tumor progression, only 5 (31%) were central or in-field. The majority (69%) of treatment failures occurred outside of the high-dose boost region, and approximately 20% of patients experienced distant failure with one failure occurring entirely outside of the original FLAIR volume. Failures were more concordant with the combined TV_{HCV}/TV_{CBV} than TV_{HCV} alone (p=0.06).

Among 22 patients who underwent correlative pre-treatment ^{11}C-MET PET imaging, the median metabolic tumor volume (MTV) was 7 cc (IQR 1–18). The median fraction of the MTV receiving 95% of the prescribed 75 Gy dose was 93% (IQR 59–100) (Figure 3). In contrast to our prior analysis[13] in which dose-intensification was based on conventional MRI-defined tumor targeting, inadequate coverage of the MTV (<95% of the MTV

receiving at least 95% of the prescribed dose) was not associated with non-central, out-of-field tumor progression (p=0.5).

Toxicity, treatment effect and salvage therapies

Ten (43%) patients experienced pseudoprogression (increase in contrast-enhancement and/or FLAIR signal intensity) a median of 3 months after chemoradiation. Four (40%) of these cases were asymptomatic, radiographic findings. Three patients required an increased dosage of steroids, and two patients required initiation of bevacizumab. One patient with a large MGMT methylated tumor encompassing the majority of the left frontal lobe experienced significant cerebral edema during radiation requiring early discontinuation of RT and tumor debulking, with subsequent significant improvement.

Grade 3+ early and late neurologic toxicities are summarized in Table 3. Fifty percent of the early events were related to cerebral edema in patients with MGMT methylated tumors, which were managed with steroids with or without bevacizumab, with clinical improvement in all patients. Two late, irreversible neurologic toxicities were observed: in a patient without radiographic changes, but with worsened seizures from baseline, and in a patient with biopsy-confirmed necrosis and worsened neurologic symptoms. No grade 5 toxicities occurred.

At progression, 12 (75%) patients received systemic therapy, either nitrosourea or alkylating chemotherapy in 58% (with or without bevacizumab), or bevacizumab alone in 42% of patients. Only 4 (25%) patients underwent resection at the time of progression, and 2 (13%) patients underwent re-irradiation.

Clinical outcomes assessment

Compliance rates for assessments at the end of radiation and 1 month after treatment were 91% and 83%, respectively, and only 52% by 7 months post-treatment, consistent with similar studies.[27]

Quality of life and symptoms—One month post-treatment, 26% of patients experienced deterioration in global quality of life, and 26% of patients experienced deterioration in symptom burden and symptom interference, with a similar distribution between mood and activity-related symptoms (Supplemental Table 1). Rates of deterioration generally remained stable by 7 months post-treatment, with deterioration in global QOL in 33% of patients, symptom burden 9%, and symptom interference 27%, although the low compliance rates may have biased results at this time point.

Neurocognitive function—A minority of patients experienced deterioration in learning and memory (5%), verbal fluency (16%), processing speed (5%) and executive function (16%) at 1 month post-treatment that remained generally stable at 7 months (Supplemental Table 1). Overall, the rates of deterioration at 1 and 7 months post-treatment in both subjective assessments as well as objective neurocognitive testing were similar to standard therapy.[27]

Discussion

We demonstrate evidence of the potential benefit and safety of a dose-intensification strategy using a biologically-informed advanced MRI technique to identify and target adversely prognostic hypercellular and hyperperfused tumor regions in patients with newly-diagnosed GBM. Early response assessment using this advanced imaging approach enabled stratification of patient outcome that superceded conventional response assessment after treatment, underscoring the more widespread diagnostic potential of this imaging strategy after chemoradiation. The minority of tumor recurrences observed in the high-dose region and relative infrequency of irreversible late CNS toxicity suggests that there is further potential to improve the therapeutic ratio, particularly if the suboptimal responders could be identified earlier during their treatment course.

While radiation dose-escalation appears to alter the pattern of tumor recurrence in patients with GBM and effectively reduces rates of early tumor progression in the regions of highest dose[13, 29], the vast majority of studies have utilized conventional, anatomic MR imaging techniques to identify and target tumor. Yet the limitations of anatomic imaging have been well recognized by numerous studies demonstrating that tumor extending outside of conventionally identified MRI predicts patient prognosis independent of T1-Gd, T2-FLAIR, and other clinical factors.[30, 31] Studies of directed stereotactic biopsy or resection of anatomic and advanced MRI and PET-defined GBM demonstrate that tumor significantly extends outside of T1-enhanced regions.[32–35] Incomplete resection or insufficient radiotherapy coverage of tumor unrecognized by anatomic MRI and identified by proton MR spectroscopy, DW-MRI, elevated CBV maps and ^{11}C-MET PET are associated with tumor recurrence, worse PFS and/or OS.[11, 13, 15, 32]

Despite the amount of evidence that anatomic MRI and targeting of T1-enhanced tumor regions is insufficient, and that highly prognostic advanced imaging techniques are promising in preliminary studies, these techniques have not been translated into standard treatment. While a limited number of centers in the U.S. with robust technical expertise are currently investigating the application of individual advanced imaging techniques including proton MR spectroscopy, ^{18}F-FDOPA PET and ^{11}C-MET, their generalizability has been a challenge. Proton MR spectroscopy detects metabolic abnormalities reflective of tumor cell proliferation, which predicts PFS and OS in GBM.[36–38] While of great interest, the practical application of proton MR spectroscopy has been limited by challenges including spectral acquisition and quantification that have limited its investigation to highly specialized centers with technical expertise.[1] Similarly, ^{18}F-FDOPA and ^{11}C-MET demonstrate utility for glioma detection and for predicting recurrence and survival compared to ^{18}F-FDG PET and anatomic MRI,[39, 40] but pose significantly greater expense outside of standard workflow and are only utilized at select centers in the U.S. with expertise in complex electrophilic tracer synthesis or with on-site cyclotrons.

As a step towards generalizing the use of advanced MR imaging for radiation treatment, multiple sites including ours have investigated the utility of perfusion MRI for brain tumors patients. While voxel by voxel analysis of CBV maps estimated from DCE versus DSC MRI are comparable, the reduced geometric distortion and whole brain coverage achieved with

DCE-MRI make it more suitable for precision radiation planning.[41–45] CBV quantification in GBM provides prognostic information about recurrence and survival beyond anatomic MRI. Elevated mean relative CBV (rCBV) >1.75 in gliomas is significantly associated with shorter time to progression for both low and high grade tumors,[6] and elevated CBV, cerebral blood flow (CBF), and vascular leakage measured by K^{trans} predict OS in patients with malignant gliomas.[2, 3, 6] Even when including molecularly classified GBM subtypes, OS is still better predicted by incorporating maximum tumor CBV.[46]

Conventional DW-MRI (b=0–1000 s/mm^2) is routinely acquired in brain tumor imaging protocols for the assessment of the mobility of water molecules in the tissue microenvironment,[47] and may be used as a surrogate for tumor cellularity.[7] By increasing diffusion weighting to high b-values (i.e. b=3000 s/mm^2), diffusion signals from edema (with high diffusion coefficient) selectively decays along with signals from normal brain, allowing for specific delineation of tumor cellularity and improved diagnostic accuracy compared with conventional ADC mapping.[12] Using the combination of DCE- and high b-value DW-MRI, the most aggressive, treatment-resistant tumor may be prospectively identified that will ultimately progress in the majority of patients treated with conventional doses of RT,[12] making it a logical target for dose-intensified radiation.

In the present study, 35% of the residual postoperative tumor was non-enhancing, which was not surprising since resection, like radiation therapy, targets the enhancing disease as the presumed “highest-risk” tumor region. By targeting biologically relevant enhancing **and** non-enhancing tumor identified using this multiparametric imaging technique, we observed promising survival outcomes and a marked reduction of tumor recurrence within the highest-dose region. Interestingly, the association between inadequate high-dose coverage (95% of 75 Gy) of the MTV identified using ^{11}C-MET PET and non-central tumor recurrence observed in our prior study[13] was not observed in this study, presumably because the majority of the MTV was also treated with high-dose when targeting this hypercellular, hyperperfused tumor imaging phenotype. While a multicenter European trial utilizing ^{11}C-MET PET for tumor targeting in GBM is currently ongoing, its implementation in the U.S. would likely not be possible due to the technical limitations at most centers. Efforts to integrate advanced MRI into radiation planning processes are anticipated to be more generalizable in the U.S.

By 3 months post-chemoradiation, approximately 50% of the hypercellular, hyperperfused tumor volume identified using this multiparametric MR imaging technique was non-enhancing. Conventional response assessment using RANO criteria[24] rely on anatomic T1-weighted gadolinium enhanced and T2/FLAIR MR images, which lacks sensitivity in identifying progressive non-enhancing, treatment resistant tumor, and specificity in distinguishing increases in contrast enhancement unrelated to tumor status (inflammation, seizures, post-surgical changes, ischemia, subacute radiation effects), especially within 3 months post-radiation.[24] While numerous response assessment strategies based on anatomic, conventional MRI have been evaluated, including subtraction maps and volumetric measurements,[48–50] no strategy has been shown to reliably evaluate early tumor response predictive of survival.

Although not incorporated in the RANO criteria,[24] a number of studies have demonstrated the potential utility of advanced MRI and PET techniques for early response assessment after chemoradiation.[51–53] Many of these studies[51, 52] have focused on distinguishing tumor progression from pseudoprogression[54, 55] (transient increases in contrast enhancement soon after chemoradiation which eventually subsides without change in therapy), in the subset of patients (20–30%) demonstrating this phenotype. Limited studies[51] have investigated whether tumor **response** can be reliably detected in all patients using physiologic imaging techniques early after radiation therapy, and whether such responses correlate with long-term survival. Several studies[56, 57] have demonstrated that higher rCBV 1 month post-chemoradiation is associated with worse OS, and that decreasing diffusion[58] or larger tumor volumes with lower ADC[59, 60] are associated with worse PFS and OS 4–10 weeks after chemoradiation. In our study, measurable differences between residual hypercellular and hyperperfused tumor, even in the setting of stable enhancing and FLAIR imaging features, enabled early stratification of patients with distinct survival outcomes. If validated in a larger cohort, the widespread application of this imaging strategy would be warranted to enable more accurate and timely therapeutic decision-making including discontinuation of ineffective (and toxic) therapies, reliable assessment for clinical trial eligibility, and future implementation in other therapeutic trials as an earlier endpoint of efficacy.

Limitations of this study include its single-arm design in a small, single-institution cohort. While key prognostic factors were similarly distributed relative to the historical control comparison cohorts from RTOG 0525 and 0825 (Supplemental Table 2), with relatively higher rates of biopsy-alone and older patients in the present study, the potential for measured and unmeasured imbalances in prognostic factors requires a larger, definitive randomized trial powered for comparative assessment to validate the findings of this study.

For future study, identifying the molecular (and related phenotypic) basis for a locoregional versus distant pattern of tumor progression would enable better selection of patients potentially benefitting from a biologically-based, dose-intensified radiation treatment approach. Moreover, understanding the molecular heterogeneity underlying the observed imaging heterogeneity is the subject of an ongoing study (NCT03287063) identifying the genomic and transcriptomic signature linked to the hypercellular and hyperperfused imaging phenotype. Additionally, earlier identification of suboptimal responders even during the course of radiation may enable adaptive modification of radiation treatment to more aggressively target persistent tumor regions, a subject of future investigation. Finally, quality of life, symptoms and neurocognitive outcomes, while globally similar in our study to standard therapy, will require comparative assessment with long-term follow-up.

An ongoing cooperative group dose-escalation trial (NRG BN001) will further elucidate the safety and efficacy of dose-intensified RT using anatomically defined tumor targets based on conventional MRI. While initial results have not demonstrated a survival benefit to dose-escalated photon therapy using conventional MR imaging to target enhancing regions, the benefit of biologically informed tumor targeting capable of identifying the presence and evolution of both enhancing **and** non-enhancing disease will require a definitive study of precision radiotherapy to assess tumor heterogeneity, identify therapeutic resistance, and improve long-term outcomes.

Supplementary Material

Refer to Web version on PubMed Central for supplementary material.

Acknowledgments

Statistical support: Yilun Sun, PhD, 4417B Med Sci I, 1301 Catherine St, Ann Arbor, MI 48109. Phone 734-936-8207. yilunsun@med.umich.edu, and Matthew Schipper, PhD, Cancer Center Biostatistics M2531. 1415 Washington Heights, Ann Arbor, MI 48109. Phone 734-232-1076. mjschipp@med.umich.edu

Funding: This study was supported in part by NIH P01 CA059827, Cancer Center Support Grant P30 CA046592, Michigan Memorial Phoenix Project Grant, and Michigan Medicine Nuclear Medicine Seed Grant

References

1. Cao Y, Tseng CL, Balter JM, Teng F, Parmar HA, Sahgal A. MR-guided radiation therapy: Transformative technology and its role in the central nervous system. Neuro Oncol 2017;19:ii16-ii29.
2. Cao Y, Nagesh V, Hamstra D, et al. The extent and severity of vascular leakage as evidence of tumor aggressiveness in high-grade gliomas. Cancer Res 2006;66:8912–8917. [PubMed: 16951209]
3. Cao Y, Tsien CI, Nagesh V, et al. Survival prediction in high-grade gliomas by MRI perfusion before and during early stage of RT [corrected]. Int J Radiat Oncol Biol Phys 2006;64:876–885. [PubMed: 16298499]
4. Choi YS, Kim DW, Lee SK, et al. The added prognostic value of preoperative dynamic contrast-enhanced MRI histogram analysis in patients with glioblastoma: Analysis of overall and progression-free survival. AJNR Am J Neuroradiol 2015;36:2235–2241. [PubMed: 26338911]
5. Hirai T, Murakami R, Nakamura H, et al. Prognostic value of perfusion MR imaging of high-grade astrocytomas: Long-term follow-up study. AJNR Am J Neuroradiol 2008;29:1505–1510. [PubMed: 18556364]
6. Law M, Young RJ, Babb JS, et al. Gliomas: Predicting time to progression or survival with cerebral blood volume measurements at dynamic susceptibility-weighted contrast-enhanced perfusion MR imaging. Radiology 2008;247:490–498. [PubMed: 18349315]
7. Sugahara T, Korogi Y, Kochi M, et al. Usefulness of diffusion-weighted MRI with echo-planar technique in the evaluation of cellularity in gliomas. J Magn Reson Imaging 1999;9:53–60. [PubMed: 10030650]
8. Murakami R, Sugahara T, Nakamura H, et al. Malignant supratentorial astrocytoma treated with postoperative radiation therapy: Prognostic value of pretreatment quantitative diffusion-weighted MR imaging. Radiology 2007;243:493–499. [PubMed: 17356177]
9. Yamasaki F, Sugiyama K, Ohtaki M, et al. Glioblastoma treated with postoperative radio-chemotherapy: Prognostic value of apparent diffusion coefficient at MR imaging. Eur J Radiol 2010;73:532–537. [PubMed: 19250783]
10. Saksena S, Jain R, Narang J, et al. Predicting survival in glioblastomas using diffusion tensor imaging metrics. J Magn Reson Imaging 2010; 32:788–795. [PubMed: 20882608]
11. Pramanik P, Parmar H, Mammoser A, et al. Hypercellularity components of glioblastoma identified by high b-value diffusion-weighted imaging. Int J Radiat Oncol Biol Phys 2015;92:811–819. [PubMed: 26104935]
12. Wahl D, Kim M, Aryal M, et al. Combining perfusion and high b-value diffusion MRI to inform prognosis and predict failure patterns in glioblastoma. Int J Radiat Oncol Biol Phys 2018;102:757–764. [PubMed: 29980414]
13. Tsien C, Brown D, Normolle D, et al. Concurrent temozolomide and dose-escalated intensity-modulated radiation therapy in newly diagnosed glioblastoma. Clin Cancer Res 2012;18:273–279. [PubMed: 22065084]
14. Kim M, Parmar H, Aryal M, et al. Developing a pipeline for multiparametric MRI-guided radiation therapy: Initial results from a phase II clinical trial in newly diagnosed glioblastoma. Tomography 2019;5: 118–126. [PubMed: 30854449]

15. Lee I, Piert M, Gomez-Hassan D, et al. Association of 11C-methionine PET uptake with site of failure after concurrent temozolomide and radiation for primary glioblastoma multiforme. Int J Radiat Oncol Biol Phys 2009;73:479–485. [PubMed: 18834673]
16. Cao Y, Shen Z. SU-FF-J-117: Integrated software tools for multi-modality functional images in cancer clinical trials. Med Phys 2007; 34.
17. Nayak L, DeAngelis LM, Brandes AA, et al. The Neurologic Assessment in Neuro-Oncology (NANO) scale: A tool to assess neurologic function for integration into the Response Assessment in Neuro-Oncology (RANO) criteria. Neuro Oncol 2017;19:625–635. [PubMed: 28453751]
18. Armstrong TS, Mendoza T, Gning I, et al. Validation of the M.D. Anderson Symptom Inventory Brain Tumor Module (MDASI-BT). J Neurooncol 2006;80:27–35. [PubMed: 16598415]
19. Efficace F, Bottomley A. Health related quality of life assessment methodology and reported outcomes in randomised controlled trials of primary brain cancer patients. Eur J Cancer 2002;38:1824–1831. [PubMed: 12204663]
20. Taphoorn MJ, Claassens L, Aaronson NK, et al. An international validation study of the EORTC brain cancer module (EORTC QLQ-BN20) for assessing health-related quality of life and symptoms in brain cancer patients. Eur J Cancer 2010;46:1033–1040. [PubMed: 20181476]
21. Benedict RHB, Schretlen D, Groninger L, Brandt J. Hopkins Verbal Learning Test–Revised: Normative data and analysis of inter-form and test-retest reliability. Clin Neuropsychol 1998;12:43–55.
22. Reitan R, Wolfson D. The Halstead–Reitan Neuropsychological Test Battery: Therapy and clinical interpretation. Middletown, MD: Neuropsychology Press; 1993.
23. Benton A, Hamsher K. Multilingual aphasia examination. 2nd ed. Iowa City, IA: AJA Associates; 1976.
24. Wen PY, Macdonald DR, Reardon DA, et al. Updated response assessment criteria for high-grade gliomas: Response Assessment in Neuro-Oncology working group. J Clin Oncol 2010;28:1963–1972. [PubMed: 20231676]
25. Gilbert MR, Wang M, Aldape KD, et al. Dose-dense temozolomide for newly diagnosed glioblastoma: A randomized phase III clinical trial. J Clin Oncol 2013;31:4085–4091. [PubMed: 24101040]
26. Gilbert MR, Dignam JJ, Armstrong TS, et al. A randomized trial of bevacizumab for newly diagnosed glioblastoma. N Engl J Med 2014; 370:699–708. [PubMed: 24552317]
27. Armstrong TS, Wefel JS, Wang M, et al. Net clinical benefit analysis of Radiation Therapy Oncology Group 0525: A phase III trial comparing conventional adjuvant temozolomide with dose-intensive temozolomide in patients with newly diagnosed glioblastoma. J Clin Oncol 2013;31:4076–4084. [PubMed: 24101048]
28. Jacobson NS, Truax P. Clinical significance: A statistical approach to defining meaningful change in psychotherapy research. J Consult Clin Psychol 1991;59:12–19. [PubMed: 2002127]
29. Kim MM, Speers C, Li P, et al. Dose-intensified chemoradiation is associated with altered patterns of failure and favorable survival in patients with newly diagnosed glioblastoma. J Neurooncol 2019;143: 313–319. [PubMed: 30977058]
30. Cao Y, Sundgren PC, Tsien CI, Chenevert TT, Junck L. Physiologic and metabolic magnetic resonance imaging in gliomas. J Clin Oncol 2006;24:1228–1235. [PubMed: 16525177]
31. Cordova JS, Shu HK, Liang Z, et al. Whole-brain spectroscopic MRI biomarkers identify infiltrating margins in glioblastoma patients. Neuro Oncol 2016;18:1180–1189. [PubMed: 26984746]
32. Pirotte BJ, Levivier M, Goldman S, et al. Positron emission tomography-guided volumetric resection of supratentorial high-grade gliomas: A survival analysis in 66 consecutive patients. Neurosurgery 2009;64:471–481; discussion 481. [PubMed: 19240609]
33. Barajas RF Jr., Phillips JJ, Parvataneni R, et al. Regional variation in histopathologic features of tumor specimens from treatment-naive glioblastoma correlates with anatomic and physiologic MR imaging. Neuro Oncol 2012;14:942–954. [PubMed: 22711606]
34. Di Costanzo A, Scarabino T, Trojsi F, et al. Multiparametric 3T MR approach to the assessment of cerebral gliomas: Tumor extent and malignancy. Neuroradiology 2006;48:622–631. [PubMed: 16752135]

35. McKnight TR, von dem Bussche MH, Vigneron DB, et al. Histopathological validation of a three-dimensional magnetic resonance spectroscopy index as a predictor of tumor presence. J Neurosurg 2002;97:794–802. [PubMed: 12405365]
36. Li X, Jin H, Lu Y, Oh J, Chang S, Nelson SJ. Identification of MRI and 1H MRSI parameters that may predict survival for patients with malignant gliomas. NMR Biomed 2004;17:10–20. [PubMed: 15011246]
37. Oh J, Henry RG, Pirzkall A, et al. Survival analysis in patients with glioblastoma multiforme: Predictive value of choline-to-N-acetylaspartate index, apparent diffusion coefficient, and relative cerebral blood volume. J Magn Reson Imaging 2004;19:546–554. [PubMed: 15112303]
38. Li Y, Lupo JM, Parvataneni R, et al. Survival analysis in patients with newly diagnosed glioblastoma using pre- and postradiotherapy MR spectroscopic imaging. Neuro Oncol 2013;15:607–617. [PubMed: 23393206]
39. Chen W, Silverman DH, Delaloye S, et al. 18F-FDOPA PET imaging of brain tumors: Comparison study with 18F-FDG PET and evaluation of diagnostic accuracy. J Nucl Med 2006;47:904–911. [PubMed: 16741298]
40. Bell C, Dowson N, Puttick S, et al. Increasing feasibility and utility of (18)F-FDOPA PET for the management of glioma. Nucl Med Biol 2015;42:788–795. [PubMed: 26162582]
41. Shiroishi MS, Castellazzi G, Boxerman JL, et al. Principles of T2 *-weighted dynamic susceptibility contrast MRI technique in brain tumor imaging. J Magn Reson Imaging 2015;41:296–313. [PubMed: 24817252]
42. Haroon HA, Patankar TF, Zhu XP, et al. Comparison of cerebral blood volume maps generated from T2) and T1 weighted MRI data in intra-axial cerebral tumours. Br J Radiol 2007;80:161–168. [PubMed: 17303617]
43. Cao Y. The promise of dynamic contrast-enhanced imaging in radiation therapy. Semin Radiat Oncol 2011;21:147–156. [PubMed: 21356482]
44. Teo QQ, Thng CH, Koh TS, Ng QS. Dynamic contrast-enhanced magnetic resonance imaging: Applications in oncology. Clin Oncol (R Coll Radiol) 2014;26:e9–e20. [PubMed: 24931594]
45. Griffith B, Jain R. Perfusion imaging in neuro-oncology: Basic techniques and clinical applications. Radiol Clin North Am 2015;53:497–511. [PubMed: 25953286]
46. Jain R, Poisson L, Narang J, et al. Genomic mapping and survival prediction in glioblastoma: Molecular subclassification strengthened by hemodynamic imaging biomarkers. Radiology 2013;267:212–220. [PubMed: 23238158]
47. Ellingson BM, Bendszus M, Boxerman J, et al. Consensus recommendations for a standardized brain tumor imaging protocol in clinical trials. Neuro Oncol 2015;17:1188–1198. [PubMed: 26250565]
48. Galanis E, Buckner JC, Maurer MJ, et al. Validation of neuroradiologic response assessment in gliomas: Measurement by RECIST, two-dimensional, computer-assisted tumor area, and computer-assisted tumor volume methods. Neuro Oncol 2006;8:156–165. [PubMed: 16533757]
49. Shah GD, Kesari S, Xu R, et al. Comparison of linear and volumetric criteria in assessing tumor response in adult high-grade gliomas. Neuro Oncol 2006;8:38–46. [PubMed: 16443946]
50. Warren KE, Patronas N, Aikin AA, Albert PS, Balis FM. Comparison of one-, two-, and three-dimensional measurements of childhood brain tumors. J Natl Cancer Inst 2001;93:1401–1405. [PubMed: 11562391]
51. Shiroishi MS, Boxerman JL, Pope WB. Physiologic MRI for assessment of response to therapy and prognosis in glioblastoma. Neuro Oncol 2016;18:467–478. [PubMed: 26364321]
52. Leao DJ, Craig PG, Godoy LF, Leite CC, Policeni B. Response assessment in neuro-oncology criteria for gliomas: Practical approach using conventional and advanced techniques. AJNR Am J Neuroradiol 2020;41:10–20.
53. Albert NL, Weller M, Suchorska B, et al. Response Assessment in Neuro-Oncology working group and European Association for Neuro-Oncology recommendations for the clinical use of PET imaging in gliomas. Neuro Oncol 2016;18:1199–1208. [PubMed: 27106405]
54. Brandsma D, Stalpers L, Taal W, Sminia P, van den Bent MJ. Clinical features, mechanisms, and management of pseudoprogression in malignant gliomas. Lancet Oncol 2008;9:453–461. [PubMed: 18452856]

55. de Wit MC, de Bruin HG, Eijkenboom W, Sillevis Smitt PA, van den Bent MJ. Immediate post-radiotherapy changes in malignant glioma can mimic tumor progression. Neurology 2004;63:535–537. [PubMed: 15304589]

56. Bag AK, Cezayirli PC, Davenport JJ, et al. Survival analysis in patients with newly diagnosed primary glioblastoma multiforme using pre- and post-treatment peritumoral perfusion imaging parameters. J Neurooncol 2014;120:361–370. [PubMed: 25098699]

57. Mangla R, Singh G, Ziegelitz D, et al. Changes in relative cerebral blood volume 1 month after radiation-temozolomide therapy can help predict overall survival in patients with glioblastoma. Radiology 2010; 256:575–584. [PubMed: 20529987]

58. Hamstra DA, Galban CJ, Meyer CR, et al. Functional diffusion map as an early imaging biomarker for high-grade glioma: Correlation with conventional radiologic response and overall survival. J Clin Oncol 2008;26:3387–3394. [PubMed: 18541899]

59. Ellingson BM, Cloughesy TF, Lai A, Nghiemphu PL, Liau LM, Pope WB. Quantitative probabilistic functional diffusion mapping in newly diagnosed glioblastoma treated with radiochemotherapy. Neuro Oncol 2013;15:382–390. [PubMed: 23275575]

60. Ellingson BM, Cloughesy TF, Zaw T, et al. Functional diffusion maps (fDMs) evaluated before and after radiochemotherapy predict progression-free and overall survival in newly diagnosed glioblastoma. Neuro Oncol 2012;14:333–343. [PubMed: 22270220]

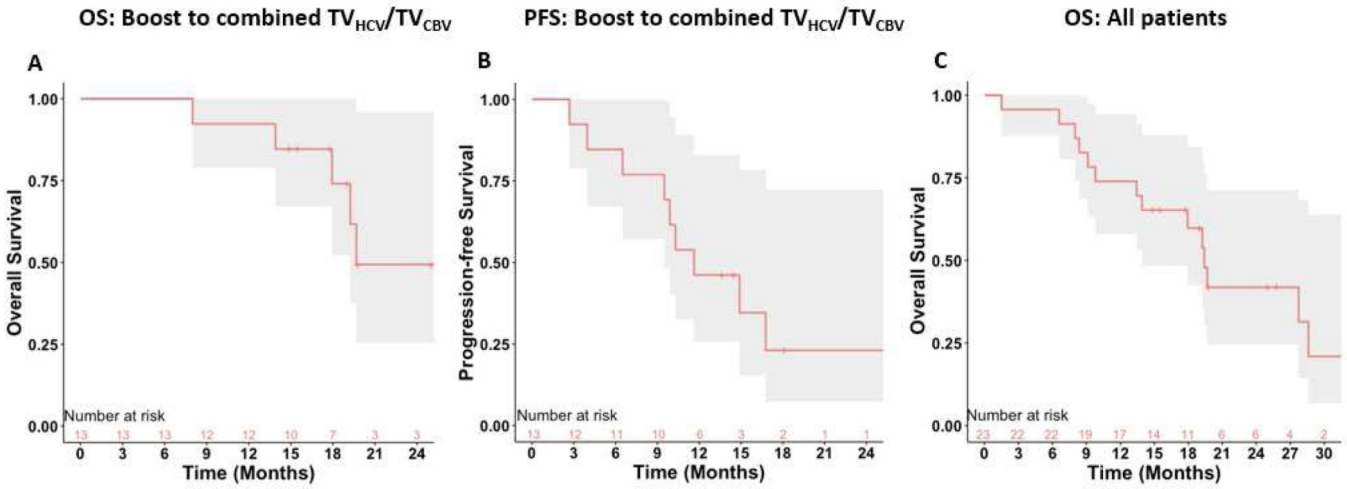

Figure 1.

Kaplan-Meier survival curves for A. Overall survival (OS) among patients undergoing dose-intensified targeting of the combined hypercellular (TV_{HCV}) and hyperperfused (TV_{CBV}) tumor (n=13) B. Progression-free survival (PFS) among patients undergoing dose-intensified targeting of the combined hypercellular and hyperperfused tumor (n=13) C. Overall survival among all patients (n=23)

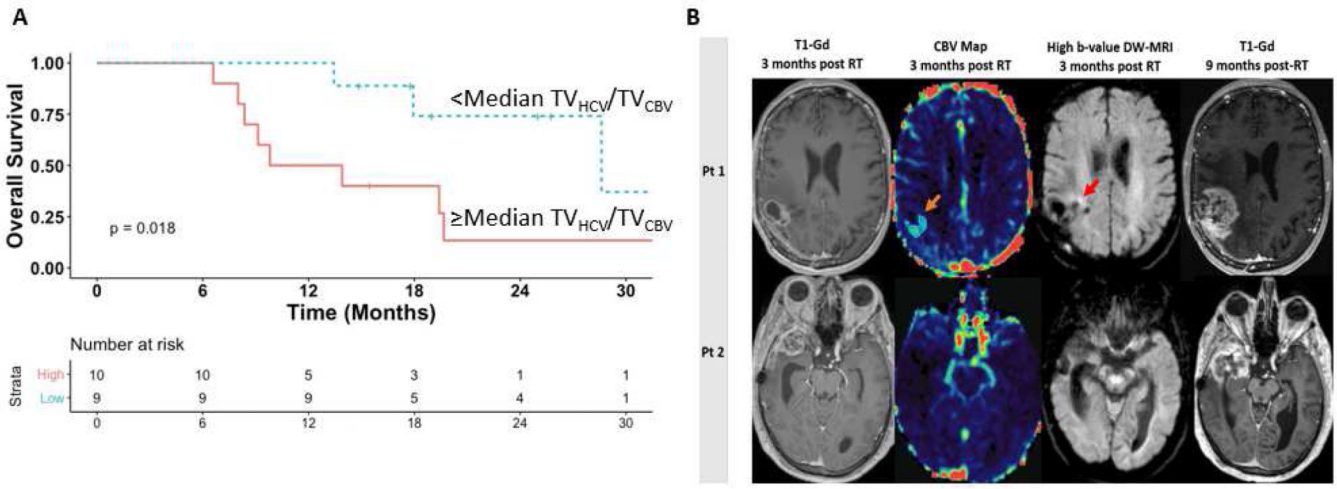

Figure 2.

Panel A. Kaplan-Meier curves for overall survival demonstrating significantly improved outcomes among patients with <median residual hypercellular/hyperperfused tumor volumes versus ≥median 3 months post-chemoradiation. Panel B. At 3 months post-radiation, standard contrast-enhanced MRI in 2 different patients (left column) was interpreted as stable disease and the patients were continued on maintenance temozolomide. Persistent hyperperfused tumor (TV_{CBV} orange arrow, 2nd column) and hypercellular tumor (TV_{HCV} red arrow, 3rd column) is detectable medially using multiparametric MRI at this time point in patient 1. In contrast, patient 2 did not have persistent residual hyperperfused/hypercellular disease. Approximately six months later, both patients developed asymptomatic worsening of their contrast-enhanced MRI prompting resection. Patient 1 had pathologically confirmed tumor progression. Patient 2 had gliosis/inflammation without residual tumor. Gd=Gadolinium; CBV=Cerebral blood volume; DW-MRI=Diffusion-weighted magnetic resonance imaging; RT=Radiation therapy

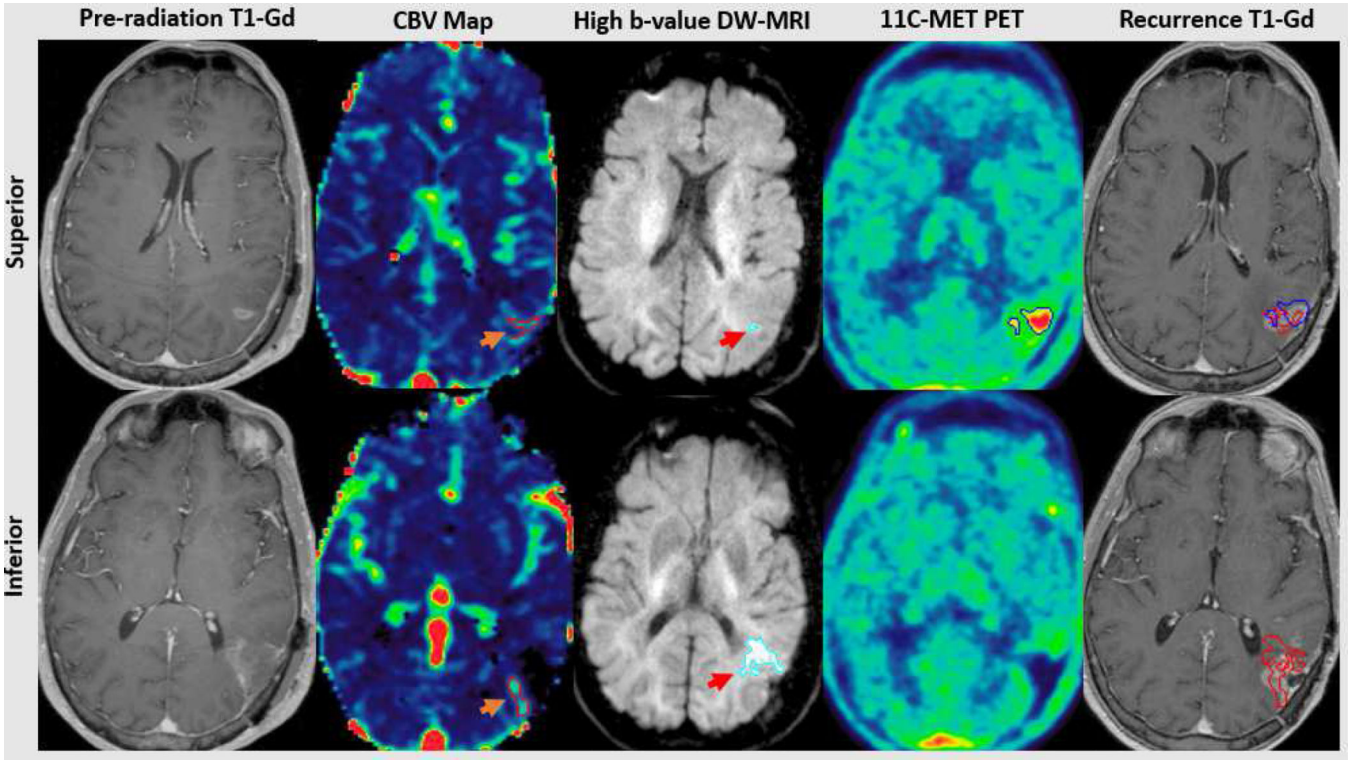

Figure 3.

Following apparent gross total resection (contrast-enhanced MRI, far left), residual tumor is demonstrated adjacent to the superior and inferior portions of the cavity. The superior residual consists of hyperperfused (orange arrow, top 2nd panel) and a small volume of hypercellular tumor (red arrow, top 3rd panel), concordant with a region of metabolic abnormality detected using ^{11}C-Methionine PET (top 4th panel). The inferior residual consists of predominantly hypercellular (red arrow, bottom 3rd panel) and some hyperperfused tumor (orange arrow, bottom 2nd panel), without associated metabolic abnormality (bottom 4th panel). Pathologically confirmed central tumor recurrence was concordant with all 3 advanced imaging tumor volumes superiorly (red and blue, upper far right panel) and the hypercellular/hyperperfused tumor inferiorly (red, bottom far right panel). Gd=Gadolinium; CBV=Cerebral blood volume; MET-PET=Methionine Positron Emission Tomography

Table 1.

Baseline characteristics of all patients and the subset of patients treated to the combined hypercellular/hyperperfused tumor

	All Patients (%)	Patients treated with targeting of hypercellular/hyperperfused tumor (%)
Count		
N	23	13
Age		
Median (Interquartile range)	61 (56, 66)	59 (56, 65)
Gender		
Female	7 (30)	5 (39)
Male	16 (70)	8 (61)
Race		
White	21 (92)	12 (92)
Black or African American	1 (4)	1 (8)
Asian	1 (4)	0 (0)
ECOG * Performance Status		
0	5 (22)	3 (23)
1	17 (74)	9 (69)
2	1 (4)	1 (8)
Baseline Neurologic Status †		
Normal	9 (39)	5 (38)
Mild	12 (52)	7 (54)
Moderate	2 (9)	1 (8)
Severe	0 (0)	0 (0)
Extent of Surgery		
Gross total resection	13 (57)	8 (62)
Subtotal resection	7 (30)	3 (23)
Biopsy	3 (13)	2 (15)
MGMT ‡ Methylation Status		
Positive	5 (22)	3 (23)
Negative	18 (78)	10 (77)
IDH€ Mutation Status		
Mutant	0 (0)	0 (0)
Wild-Type	22 (96)	13 (100)
Unknown	1 (4)	0 (0)
Tumor laterality		
Right	8 (35)	5 (38)
Left	15 (65)	8 (62)
Tumor location		

	All Patients (%)	Patients treated with targeting of hypercellular/hyperperfused tumor (%)
Frontal	11 (48)	7 (54)
Temporal	7 (30)	3 (23)
Parietal	2 (9)	2 (15)
>1 lobe	3 (13)	1 (8)
Handedness		
Right	20 (87)	11 (85)
Left	3 (13)	2 (15)
Education		
≤ 12 years	4 (17)	1 (8)
>12 years	19 (83)	12 (92)

*ECOG = Eastern Cooperative Oncology Group;

†Using the Neurologic Assessment in Neuro-Oncology (NANO) Scale, defined as at least 1 neurologic function deficit of the specified severity in at least 1 domain;

‡MGMT = O^6-methylguanine-DNA methyltransferase; €IDH = Isocitrate dehydrogenase

Table 2.

Summary of Anatomic and Advanced Imaging Volumes Pre- and Post-Radiation

Median	Pre-radiation (IQR*) N=23	3-Month Post-RT† (IQR) N=19	Change (cc) (IQR)	Change (%) (IQR)
Enhancing tumor volume‡ (cc)	16.9 (10.5, 33.5)	10.4 (3.5, 15.6)	−3.0 (−9.5, 0.0)	−28 (−72, 0)
Hypercellular tumor volume (TV_{HCV}, cc)	6.0 (4.3, 10.8)	1.1 (0.0, 8.6)	−3.5 (−5.8, −1.7)	−81 (−100, −46)
Hyperperfused tumor volume (TV_{CBV}, cc)	4.5 (1.8, 9.9)	1.1 (0.6, 3.9)	−1.4 (−4.3, 0.0)	−63 (−87, 0)
Combined Union of TV_{HCV}/TV_{CBV} (cc)	11.4 (6.6, 20.0)	3.0 (1.0, 12.1)	−5.0 (−6.9, −0.4)	−60 (−88, −2)
Overlap of TV_{HCV}/TV_{CBV} (cc)	0.5 (0.0, 1.1)	0.0 (0.0, 0.2)	−0.2 (−0.5, 0.0)	−78 (−98, −32)
Non-enhancing TV_{HCV} (cc)	2.1 (1.5, 3.5)	1.4 (0.0, 2.8)	−0.7 (−1.9, 0.1)	−33 (−90, 4)
Non-enhancing TV_{CBV} (cc)	1.7 (0.6, 2.8)	0.8 (0.5, 1.5)	−0.3 (−1.3, 0.2)	−30 (−70, 30)
Non-enhancing Union of TV_{HCV}/TV_{CBV} (cc)	3.7 (2.4, 5.9)	2.1 (0.8, 6.0)	−1.2 (−2.9, 0.6)	−29 (−79, 8)
Non-enhancing Union of TV_{HCV}/TV_{CBV} (%)	35.5 (24.6, 57.4)	52.1 (27.6, 71.4)	3.4 (−6.4, 29.4)	16 (−20, 72)

*IQR=Interquar le range;

†RT=Radia on therapy;

‡Excluding surgical cavity

Int J Radiat Oncol Biol Phys. Author manuscript; available in PMC 2022 July 01.

Table 3.

Summary of grade 3 or higher neurologic toxicities

		Early (<6 months post-chemoradiation)			
Patient	**MGMT* methylation status**	**Type**	**Grade**	**Interval from RT† (months)**	**Treatment**
1	Negative	Seizure, worsened hemiparesis, imbalance	3	0.6	Steroids
2	Positive	Worsened gait, sensory neglect	3	3	Steroids, bevacizumab
3	Negative	Worsened hemiparesis and gait	3	3	Steroids, bevacizumab
4	Positive	Seizure, aphasia, worsened hemiparesis	4	During RT	Steroids, debulking surgery
Late (>6 months post-chemoradiation)					
5	Negative	Seizures	3	10	Bevacizumab
6	Positive	Hemiparesis, worsened gait and word-finding difficulty	3	17	Bevacizumab

*MGMT = O^6-methylguanine-DNA methyltransferase;

†RT=radiation therapy